

Article

Effect of Oxidative Roasting on Selective Leaching of Lithium from Industrially Shredded Lithium Iron Phosphate Blackmass

Ayesha Tasawar ^{1,*}, Daniel Dotto Munchen ², Alexander Birich ² , Rungsima Yeetsorn ¹  and Bernd Friedrich ² 

¹ The Sirindhorn International Thai German Graduate School of Engineering, King Mongkut's University of Technology North Bangkok, Bangkok 10800, Thailand; rungsima.y@tggs.kmutnb.ac.th

² IME Process Metallurgy and Metal Recycling, RWTH Aachen University, Intzestrasse 3, 52056 Aachen, Germany; dmunchen@metallurgie.rwth-aachen.de (D.D.M.); abirich@ime-aachen.de (A.B.); bfriedrich@ime-aachen.de (B.F.)

* Correspondence: atasawar@metallurgie.rwth-aachen.de

Abstract

The increasing need-based demand for lithium iron phosphate (LFP) batteries in electric vehicles and energy storage systems necessitates the development of efficient and sustainable recycling methods. This study investigates the effect of oxidative roasting on lithium extraction from industrially sourced LiFePO_4 (LFP) blackmass containing high graphite content (~46%) and mixed electrode materials. Roasting at 650 °C for one hour converted LiFePO_4 into water-soluble $\text{Li}_3\text{Fe}_2(\text{PO}_4)_3$ and Fe_2O_3 , while reducing carbon and fluorine levels. However, contrary to expectations, mild-acid leaching (pH 2, 40 g/L, 20 °C) of roasted blackmass did not improve lithium recovery compared to unroasted material, yielding approximately 33% extraction efficiency. Strong-acid leaching (pH 0, $\text{H}_2\text{SO}_4/\text{H}_2\text{O}_2$) achieved over 95% lithium recovery but also resulted in significant co-dissolution of iron and other impurities. Our XRD and SEM analyses showed that some lithium-containing phases remained in the residue after water leaching, while acid leaching left mainly iron oxide and graphite. These results suggest that, for complex and graphite-rich industrial blackmass, roasting may not always deliver the expected boost in lithium recovery. Our findings highlight the need to tailor recycling processes to the specific characteristics of battery waste and suggest that direct hydrometallurgical methods could be more effective for complex, impurity-rich LFP blackmass streams.

Keywords: lithium iron phosphate (LFP) batteries; hydrometallurgy; leaching; oxidative roasting; selective recovery; sustainable recycling; water leaching; black mass; acid leaching



Academic Editors: Jean François Blais and Petros E. Tsakiridis

Received: 16 May 2025

Revised: 17 June 2025

Accepted: 28 June 2025

Published: 30 June 2025

Citation: Tasawar, A.; Dotto Munchen, D.; Birich, A.; Yeetsorn, R.; Friedrich, B. Effect of Oxidative Roasting on Selective Leaching of Lithium from Industrially Shredded Lithium Iron Phosphate Blackmass. *Metals* **2025**, *15*, 739. <https://doi.org/10.3390/met15070739>

Copyright: © 2025 by the authors. Licensee MDPI, Basel, Switzerland. This article is an open access article distributed under the terms and conditions of the Creative Commons Attribution (CC BY) license (<https://creativecommons.org/licenses/by/4.0/>).

1. Introduction

The increasing demand for electric vehicles (EVs) and energy storage systems has led to a surge in the production and use of lithium-ion batteries (LIBs), particularly lithium iron phosphate (LFP) batteries [1,2]. LFP batteries have gained widespread adoption in large electric buses and cars due to their safety, long cycle life, and cost-effectiveness [3]. However, this growth will result in a significant increase in spent LIBs, with estimates suggesting that up to 340,000 tons of spent LFPs from EVs will be available for recycling annually by 2040 [1].

The recycling of spent LFP batteries is crucial from both environmental and resource recovery perspectives [4]. These batteries contain valuable metals such as lithium and phosphorous, as well as harmful materials like organic electrolytes and binders like

polyvinylidene fluoride (PVDF) that pose serious threats to ecosystems and human health if improperly disposed of [3,5,6].

Current recycling methods for LFP batteries can be broadly categorized into physical and chemical processes. Physical methods, such as mechanical separation, are often used as pretreatment steps to separate electrode materials from other battery components [7–9]. Chemical methods include pyrometallurgical and hydrometallurgical processes, each with their own advantages and limitations [10].

Pyrometallurgical processes involve high-temperature treatment to recover metals, but they often result in the loss of valuable materials like graphite and lithium, leading to significant carbon emissions [2,11,12]. Hydrometallurgical processes, on the other hand, use acid or alkaline leaching to dissolve cathode and anode materials, followed by purification steps [13–15]. While more selective, these processes can be chemically intensive and may present challenges when separating residues from leach solutions [7,16].

Recent research [17–19] has focused on improving the efficiency and sustainability of LFP battery recycling. Thermal pretreatment, or roasting, has emerged as a promising approach to enhance the recovery of valuable metals. Roasting can remove organic binders and modify the chemical structure of cathode materials, potentially improving the subsequent leaching or separation processes. However, the effects of thermal treatment on industrially shredded LFP blackmass (BM) are not yet fully understood. Factors such as roasting temperature, duration, and atmosphere can significantly impact the physical and chemical properties of the LFP blackmass [12,20]. Moreover, the optimal conditions for thermal pretreatment may vary depending on the subsequent recovery process employed. Studies indicate that the oxidative pre-treatment of LFP Blackmass at 650 °C aims to enhance lithium leaching efficiency and selectivity in the subsequent low pH water leaching process, due to the decomposition of LFP and the formation of water-soluble lithium compounds, while simultaneously reducing the dissolution of impurities like aluminum, copper, and fluorides from binder removal [12,21]. Another study [22] submitted LFP cathode material to TGA and DSC analysis under air flow and reported a weight loss of 6.68% up to 600 °C. The exothermic peaks (DSC analysis) corresponded to binder and carbon decomposition at 475 °C and 579 °C, respectively. A color change from dark to reddish brown was also observed due to the oxidation of Fe (II) to Fe (III), which is representative of the formation of Fe_2O_3 and $\text{Li}_3\text{Fe}_2(\text{PO}_4)_3$, as confirmed by XRD standard spectra and XPS analysis. This mixture was then subjected to 2.5 mol/L H_2SO_4 leaching for 2 h at 60 °C, with 100 g/L, resulting in a leaching efficiency of 97% and 98% for Li and Fe, respectively. Therefore, the process is not selective [23]. The roasted LFP virgin cathode powder in air flow for 1 h at 550 °C formed Fe_2O_3 and $\text{Li}_3\text{Fe}_2(\text{PO}_4)_3$, in which a further leaching with H_2SO_4 (0.5 M) at 60 °C for 2 h and 80 g/L has yielded more than 97% of Li recovery. This study [7] indicated that the Fe is highly leached because of the air roasting.

To achieve selective leaching, the Pourbaix diagram is also explained by Jing et al. (2019) [7], revealing that E-pH diagrams can effectively guide the selective extraction of lithium from spent LiFePO_4 . By optimizing conditions, such as high temperature, neutral pH, low redox potential, and the use of H_2O_2 as an oxidant, up to 95.4% Li recovery was achieved while minimizing Fe dissolution. This method eliminates the need for large amounts of acids or bases, offering a commercially promising and environmentally friendly approach for lithium recovery.

Therefore, the metallurgical approach of combining thermal pretreatment to better condition impurities and remove binder, electrolyte which contains F, and separators from LFP BM, followed by selective hydrometallurgical leaching has shown ways forward that are both effective and highly selective against FePO_4 in spent LFP systems.

The objectives of this study are: (1) to evaluate the impact of roasting as a pre-treatment on lithium leaching efficiency and selectivity; (2) to characterize the changes in the composition and morphology of the blackmass during roasting; and (3) to compare conventional acid-based leaching with mild-acid based leaching to assess the greener route. By examining these factors, we seek to develop a more efficient and environmentally friendly method for recycling spent LFP batteries, contributing to the circular economy of battery materials and addressing the growing challenge of battery waste management [24–26].

2. Materials and Methods

2.1. Materials Characterization

The input material was lithium iron phosphate (LFP) blackmass generated from an industrially inert shredder, in which particles greater than 1 mm were separated by sieving. All characterizations, before and after each process, consisted of:

- Chemical composition—determined by ICP-OES (Spectro CIROS Vision, Spectro Analytical Instruments GmbH, Kleve, Germany) after digestion in aqua regia;
- Carbon content—determined by combustion method for carbon analysis (ELTRA CS 2000, ELTRA GmbH, Haan, Germany);
- Fluorine content—determined by Ion Chromatography (811 Compact IC pro, Deutsche Metrohm GmbH & Co., KG, Filderstadt, Germany);
- Phases/compounds—determined by X-Ray Diffractometry (Rigaku SmartLab 9 kW, Bangkok, Thailand) with measurements every 0.5° with radiation Cu K α ;
- Morphology of particles—determined by Scanning Electron Microscopy (SEM) (JEOL model JSM-6610 LV, Bangkok, Thailand).

2.2. Roasting in Air Atmosphere

The LFP blackmass underwent an air roasting process in a rotary kiln (Carbolite Gero, TS01 11/400, Neuhausen, Germany), where the flow rate was maintained at a constant 5 L/min. A sample of 200 g of LFP blackmass was placed in a quartz tube and heated to 650 °C at a rate of 250 °C/h, and this temperature was sustained for one hour. Following the roasting process, the material was cooled to room temperature within the furnace before being removed and weighed.

2.3. Leaching Procedure

The leaching trials were conducted according to a general full factorial design, utilizing the analysis of variance (ANOVA) statistical method to evaluate the leaching efficiencies of the metals lithium (Li), iron (Fe), phosphorus (P), aluminum (Al), and copper (Cu). Figure 1a summarizes the experimental design, which considered two factors: roasting and final pH, obtained according to the leaching agent/conditions of each trial. The complete design of experiments resulted in 8 runs, each duplicated, yielding a total of 16 experiments. Both roasted and unroasted blackmass with a particle size of less than 90 μm were leached in a 250 mL glass reactor equipped with a sealed three-neck lid. Agitation was performed using a mechanical stirrer and maintained at a constant speed of 350 rpm throughout all trials. The solid/liquid ratio was set to 40 g/L, with temperature maintained at 20 °C and a duration of 90 min. The concentration of sulfuric acid (H_2SO_4) was kept constant at 2 mol/L, representing 10 times the stoichiometric excess, while hydrogen peroxide (H_2O_2) was maintained at a concentration of 2.7 mol/L. All of these factors were selected based on prior assessments. The pH was monitored using a Mettler Toledo device during the leaching processes and served as the basis for decision-making when necessary. Following the leaching process, the solid residue and solution were separated by filtration and washed once using 200 mL of distilled water. Washing after leaching removes any residual soluble

impurities, ensuring the purity of the filtrate and precipitate. Both the filtrate and residue were collected for chemical analysis. The latter was dried overnight at 95 °C. Figure 1b shows a sketch of the process flow and analysis of this study.

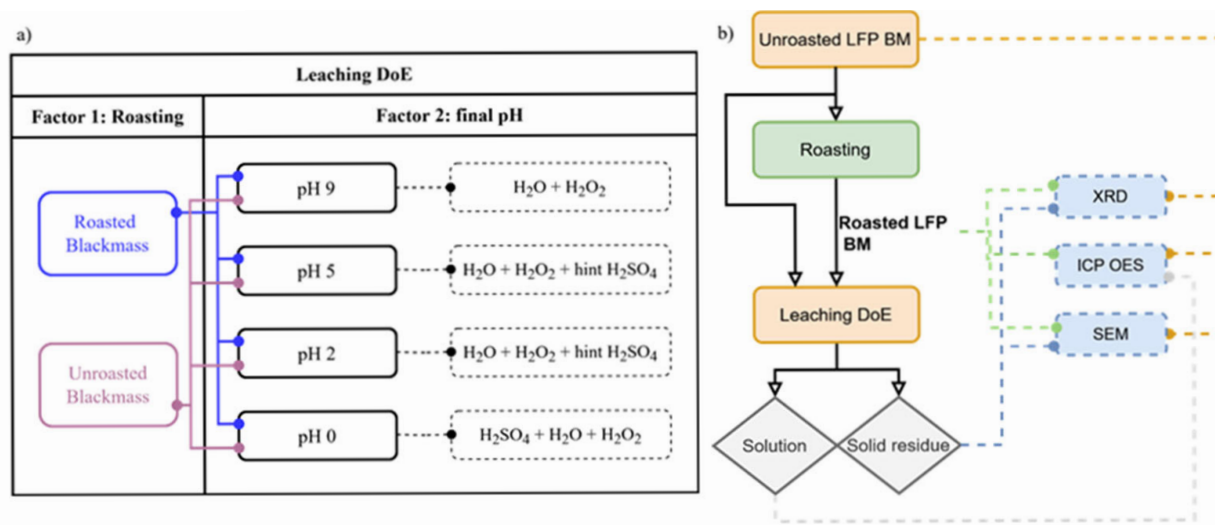


Figure 1. (a) Leaching design of experiments (DoE) and (b) process flow and analysis of this study.

The lithium leaching efficiency was calculated using the following equation;

$$\text{Leaching Efficiency (\%)} = \frac{(\text{Amount of Li dissolved in Leach Solution})}{(\text{Initial amount of Li in Blackmass})} \times 100 \quad (1)$$

where:

Amount of Li in blackmass = Li concentration in leach solution (mg/L) × Volume of leach solution (L)

Initial amount of Li dissolved in leach solution = Li content in blackmass (wt.%) × Mass of blackmass used in leaching (g)

3. Results

3.1. LFP Blackmass Characterization and Roasting Effect

The chemical composition of unroasted and roasted blackmass is shown in Figure 2. In comparison with results found in a number of studies [24,27], the composition is similar. The “others” label for both roasted and unroasted LFP blackmass refers to oxygen content and unknown metals/oxides. Based on the Li-, Fe-, and Al- content, it is possible to estimate the theoretical oxygen content. Following the assumption that all Li in the sample is in the form of LiFePO₄, the O-content is 20.1% for unroasted blackmass, which leaves 5.51% of unidentified compounds. For the roasted blackmass, the oxygen is divided into three compounds, Li₃Fe₂(PO₄)₃, Fe₂O₃, and AlPO₄ according to the literature and the XRD results from this study (Figure 3). This means that, theoretically, the O-content is 37.9%, which leaves ~2% of unidentified compounds.

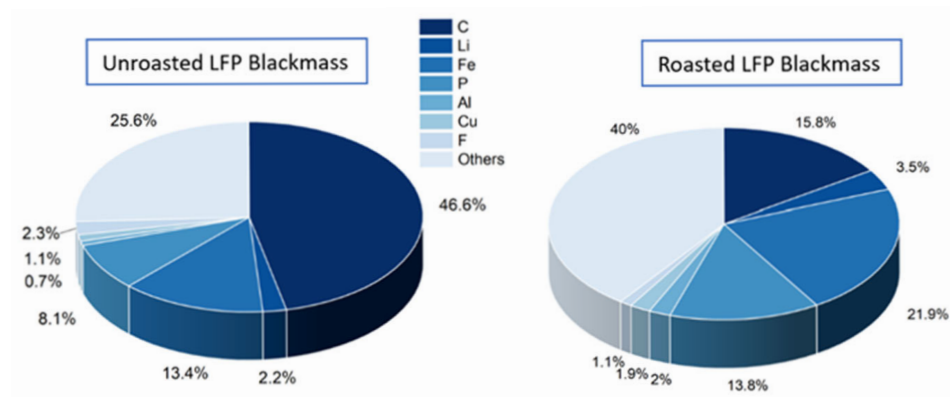


Figure 2. (Left) Elemental composition of industrially shredded LFP/graphite blackmass. (Right) Elemental composition of roasted LFP blackmass at 650°.

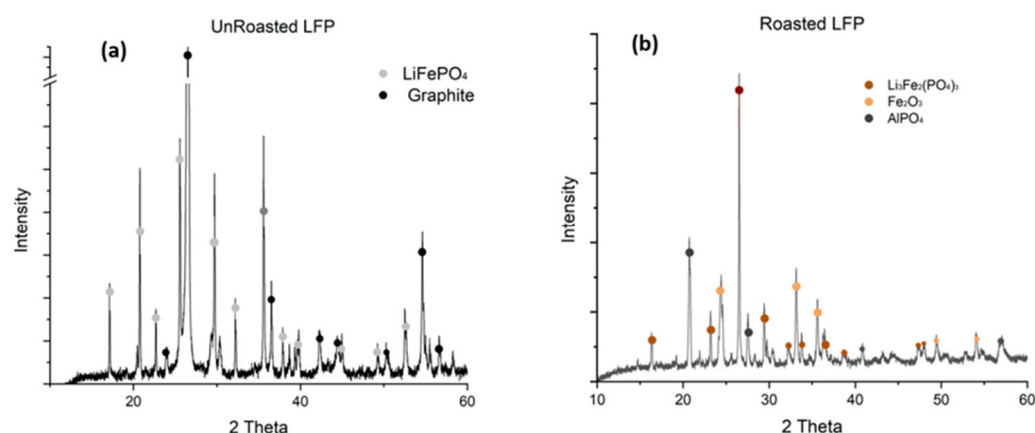


Figure 3. XRD Patterns of unroasted (a) and roasted (b) LFP blackmass.

The elemental composition analysis of the unroasted LFP/graphite blackmass reveals significant carbon content (46.6%) alongside key battery components including iron (13.4%), phosphorus (8.1%), and lithium (2.2%). The presence of aluminum (0.7%), copper (1.1%), and fluorine (2.3%) indicates industrially shredded blackmass with residual binder materials (PVDF), and possibly, traces of electrolyte. Following oxidative roasting, the carbon content dramatically decreases to 15.8% due to the conversion of graphite and carbon coatings from LFP structures. Simultaneously, the relative concentrations of active material components increase substantially, with phosphorus rising to 13.8%, iron to 21.9%, and lithium to 3.5%. The reduction in fluorine content (from 2.3% to 1.1%) demonstrates the partial decomposition of PVDF binders during thermal treatment, while the compositional shifts overall reflect successful thermal preprocessing of the blackmass for subsequent hydrometallurgical lithium extraction.

In terms of mass balance, the carbon content decreased from an initial mass of 46.6 g to 13.983 g after roasting (calculated using 15.8% multiplied by the final mass of 88.5 g), indicating that ~70% of the carbon was burned out. Similarly, the fluoride content decreased from an initial 2.26 g to 1.01 g, indicating that around 55.4% of the fluorine was removed in the off-gas.

The mineralogical compositions of the unroasted and roasted blackmass were analyzed by X-ray diffraction, as shown in Figure 3.

The XRD patterns reveal dramatic structural transformations in the blackmass following oxidative roasting treatment. In the unroasted blackmass, the diffractogram is dominated by an intense, sharp graphite reflection at approximately 26° 2θ (ICDD 00-041-1487), with relatively minor LiFePO₄ reflections, indicating the prevalence of graphite in the

initial battery waste material. After roasting at 650 °C, the graphite peak was replaced by one representing the Lithium compound, confirming successful carbon removal. Concurrently, the olivine-type orthorhombic LiFePO_4 phase transforms into $\text{Li}_3\text{Fe}_2(\text{PO}_4)_3$ (similar to ICDD Card No. 00-052-0512), as evidenced by multiple new diffraction reflections. The formation of Fe_2O_3 reflections (similar to ICDD 01-089-0596) confirms the complete oxidation of Fe(II) to Fe(III), while the appearance of AlPO_4 reflections indicates reactions involving aluminum impurities during thermal treatment. These phase transformations, particularly the conversion to $\text{Li}_3\text{Fe}_2(\text{PO}_4)_3$, could be favorable for effective lithium extraction, as this phase is supposed to exhibit significantly enhanced lithium leachability compared to the original LiFePO_4 structure. The roasting was also confirmed with the color change (Figure 4), just as reported by Wang et al., 2024 [23] and Zhang et al. [28].

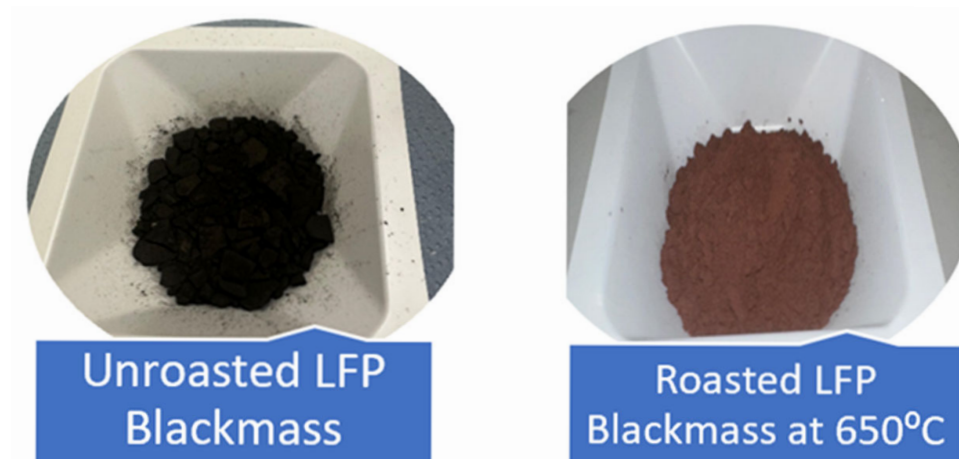


Figure 4. Color change upon oxidative roasting at 650 °C.

The loss of weight was 11% up to 650 °C, which is consistent with the findings of Lai et al., 2023 [17], Li et al., 2022 [29], and Müller et al., 2024 [24]. The first study used an LFP cathode mixed with graphite from real batteries as an input material, which demonstrated the existence of some contaminants such as Al and Cu, which revealed, after treatment in a 600 °C oxidation environment for 1 h, the presence of un-decomposed $\text{Li}_3\text{Fe}_2(\text{PO}_4)_3$, Fe_2O_3 , graphite, and LiFePO_4 .

Figure 5a displays a heterogeneous mixture where angular, bright particles (representing LiFePO_4 cathode material) are distributed among darker, fine graphite particles (anode material). While most active materials appear well-liberated, notable graphite agglomeration is observed, with fine LiFePO_4 particles adhering to graphite surfaces due to PVDF binder interactions. The particle size distribution is notably varied, with LiFePO_4 generally exhibiting larger dimensions compared to graphite components. Following oxidative roasting (Figure 5b), the microstructure demonstrates markedly improved particle liberation and reduced agglomeration, attributed to PVDF decomposition above 350 °C. The formation of distinctive rod-like particles indicates the successful oxidation of iron to Fe_2O_3 (hematite), confirming the phase transformation observed in XRD analysis. The particles exhibit clearer boundaries and improved separation, facilitating enhanced accessibility to lithium-bearing phases during leaching. These morphological changes align with the compositional transformations previously identified and suggest improved leaching kinetics for lithium recovery.

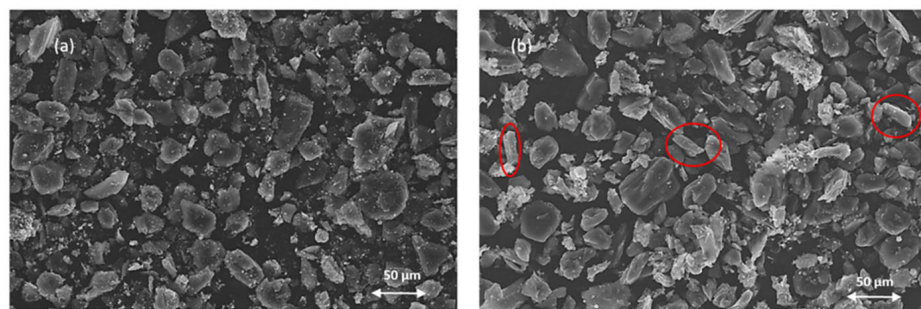


Figure 5. (a) SEM analysis of industrially shredded LFP/graphite blackmass. (b) SEM analysis of LFP blackmass roasted at 650 °C for 1 h.

3.2. Selectivity of Lithium Leaching

The purpose of using H_2O_2 in combination with an acid is to form an oxidative environment within an acidic leaching system, which several authors have already studied [7,25,28]. Such conditions allow Fe(II) from the LiFePO_4 molecule, after dissolution, to be oxidized to Fe (III). Then, the reaction with PO_4^{3-} takes place, forming FePO_4 , which is not soluble under these conditions. Consequently, Li is selectively dissolved in solution, whilst FePO_4 precipitates. In addition to the selectivity, the maximization of the Li leaching efficiency is also targeted. Both these aspects are evaluated in this section with the assistance of the analysis of variance (ANOVA) method. The leaching efficiency of the LFP BM main components was evaluated for roasted and unroasted BM at different final pH values.

The first outcome of such analysis is the significance of each factor and the interaction between them, in relation to the response, which is the leaching efficiency. The significance is measured by the calculated p -value, which is shown in Table 1 for each component. In green are the p -values lower than 0.05 (i.e., 5%), which is the common standard value in statistical analysis that defines the significance aspect in the studied system. With that in mind, the evaluation allows for the conclusion that the final pH was significant for all chemical elements, which was expected due to each individual chemical element's hydrometallurgical behavior. However, even though the final pH is very different—acid vs. low pH water leaching—the p -value provided an interesting insight: regardless of the change in this factor, the leaching efficiency of Fe, P, and Cu remains practically unchanged when the BM is roasted. The p -value of the interaction between factors also shows that the Fe and Cu leaching efficiencies are not significant, which will be addressed with the analysis of the interaction plot. The complete ANOVA statistical analysis is detailed in the Supplementary Materials.

Table 1. Calculation of p -value using ANOVA statistical method to calculate significance of each component.

p -Value	Li	Fe	P	Al	Cu
Factor 1: roasting	0.000	0.44	0.15	0.001	0.13
Factor 2: final pH	0.000	0.000	0.000	0.000	0.000
Interaction (Roasting \times Final pH)	0.000	0.54	0.01	0.000	0.31

In Figure 6 the effect of the interaction between both factors on the leaching efficiency for each LFP component is shown, where it is possible to observe in more detail what the p -values mean. For Fe and P, in red and blue, respectively, it is possible to observe that when the BM is roasted, at three final pH values, the increase or decrease of leaching efficiency is practically negligible, with the exception of the final pH, 0, at which a sharp

decrease is observed for P in the unroasted BM. This is the reason both these components showed p -values higher than 0.05. The same is observed for Cu, but at a final pH of ~2.

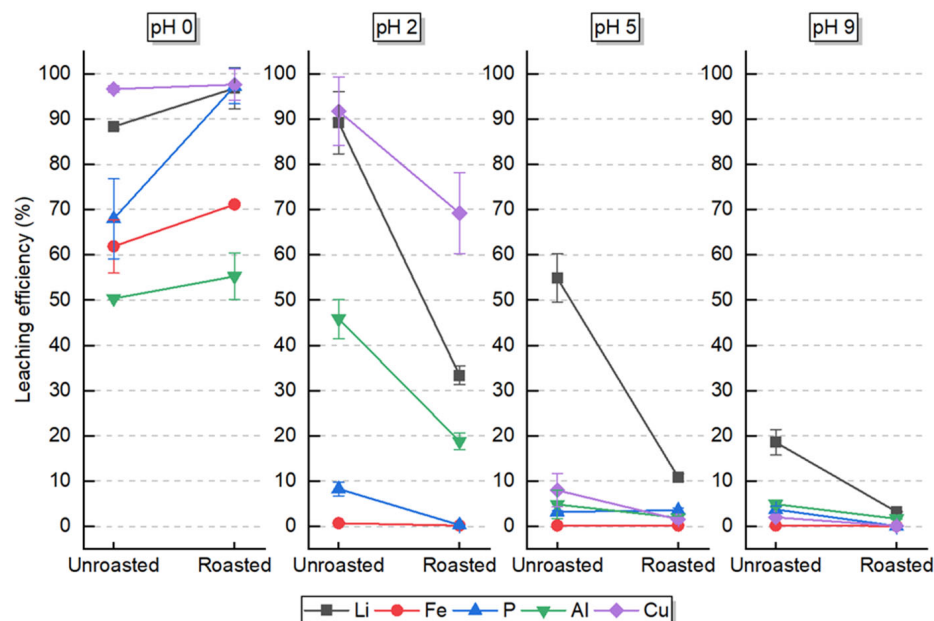


Figure 6. Leaching efficiencies (%) of Li, Fe, P, Al, and Cu in different leaching environments indicated by pH 0, 2, 5, and 9.

The other interactions between factors show a p -value lower than 0.05, which is significant and can be seen in Figure 6 with great variations of leaching efficiency. When both roasted and unroasted BM are leached at pH 9, a poor leaching efficiency of less than 20% is observed. Nonetheless, a slight selectivity for Li compared to other elements can be observed for unroasted BM (molar ratio of Li/Fe is 47.2). According to the E-pH diagram for the unroasted LPF system, Li_3PO_4 could be formed, which indeed presents very low solubility [5,30,31]. Moreover, even though there is no information about the solubility of $\text{Li}_3\text{Fe}_2(\text{PO}_4)_3$, these results suggest that its solubility is not reached in such conditions of 40 g/L and 20 °C. However, it was reported that roasted virgin LFP material achieved 33% Li leaching efficiency in water with a higher S/L ratio (80 g/L) and temperature (60 °C), whilst the Fe leaching efficiency was negligible [23]. A similar behavior is observed at pH 5, where a hint of H_2SO_4 was used (approximately 5 mL, 2 mol/L), but with a greater selectivity for the unroasted BM. However, the leaching efficiency of Li reached only 33% against less than 8% for Cu, which is still unsatisfactory for achieving the EU goals [32], for example.

At pH 0, the behavior of the five chemical elements is completely the opposite: the leaching efficiencies are higher than 50% for all chemical elements in both roasted and unroasted BM, which demonstrates a poor level of selectivity of Li against the other elements (molar ratio of Li/Fe is 1.86). Although, it can be observed that the roasted BM showed higher leaching efficiency for all elements, especially for P. Cu is probably unaffected by the roasting, which is dissolved at pH 0 [33]. With an unknown pH, but 500 °C-roasted BM, and leaching conditions of 100 g/L, 60 °C for 40 min, and 0.8 mol/L H_2SO_4 , one study [18] showed a lower leaching efficiency, possibly due to the formation of more stable oxide structures at higher temperatures. Yang et al., 2021 [34] also reported a decrease in leaching efficiency when the roasting was performed in an oxidizing environment, although it was not significant, which suggests that the leaching of Fe became difficult.

The selectivity of Li against Fe and P, combined with a high leaching efficiency of 90%, is only observed at pH 2 for unroasted BM, where a hint of H_2SO_4 was added controllably

(approx. 10 mL). In this situation, Al and Cu also showed considerably high leaching efficiencies. However, the final concentration in solution of both these metals is 7 times lower than the concentration of Li, circa 180 mg/L, which could facilitate further refinement.

In general, unroasted BM showed higher leaching efficiencies than roasted BM for all components. Since no data were found for the solubility of $\text{Li}_3\text{Fe}_2(\text{PO}_4)_3$, it is suggested that this compound is insoluble at mild pH values. In addition, for the roasted BM, most of the Fe(II) from LiFePO_4 is oxidized, forming Fe_2O_3 , which is not leached easily even by strong acid media [24]. On the other hand, LiAlO_2 could also be formed during the roasting of the BM, which is a compound known to be indissoluble [27,28].

Another important aspect that adds error is possibly the presence of a binder, separators, and electrolyte of LFP batteries on the unroasted BM. The residues of organic matter could encapsulate the LFP particles, hindering the leaching process. This is observed through the presence of fluorine from the electrolyte. In the unroasted BM, the content is 2.26 wt.% compared to only 1.14 wt.% in the roasted BM.

3.3. Characterization of Solid Residues

The solid residues (cakes) obtained after leaching were analyzed using XRD and SEM techniques to understand the phase composition changes resulting from the combined oxidative roasting and leaching treatments. This section compares the outcomes of selective mild-acid leaching (pH 2) versus strong acid leaching (pH 0).

SEM analysis reveals striking differences in particle morphology between the two leaching methods. In the mild-acid leaching residue (pH 2), numerous fine white particles remain visible on the surfaces of larger particles, as shown in Figure 7a. This indicates that water-soluble lithium compounds, particularly $\text{Li}_3\text{Fe}_2(\text{PO}_4)_3$, persist in the residue after mild-acid leaching. In contrast, the acid-leached sample (pH 0) shows a cleaner surface with complete removal of these white particles. Instead, we observe the formation of distinctive rod-like spherical crystalline structures of Fe_2O_3 alongside graphite particles, which constitute most of the precipitate.

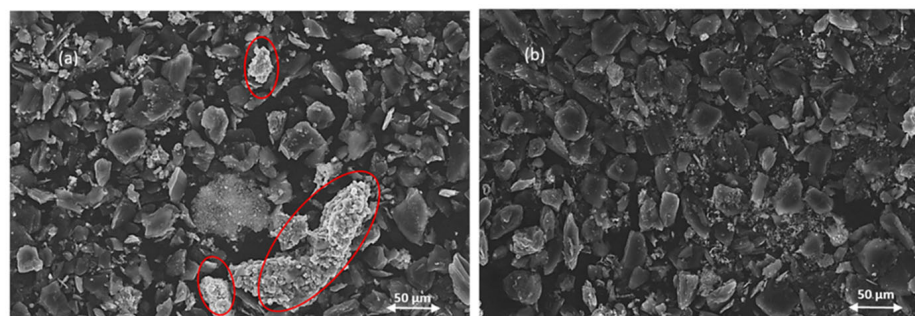


Figure 7. (a) Mild-acid-leaching residue pH 2 (presence of un-leached agglomerated Li compound). (b) Acid-leaching residue pH 0.

The XRD patterns provide further confirmation of these observations. Figure 8a shows that the mild-acid-leaching residue still contains significant amounts of water-soluble $\text{Li}_3\text{Fe}_2(\text{PO}_4)_3$, demonstrating incomplete lithium extraction under mild pH 2 conditions. The presence of Fe_2O_3 reflections confirms that the roasting treatment at 650 °C for 1 h successfully oxidized Fe (II) to Fe (III), transforming the original LiFePO_4 structure. In contrast, Figure 8b shows that the acid-leaching residue contains only graphite and minor Fe_2O_3 reflections, with no detectable lithium-containing compounds, indicating a highly efficient lithium recovery through acid leaching of the roasted blackmass.

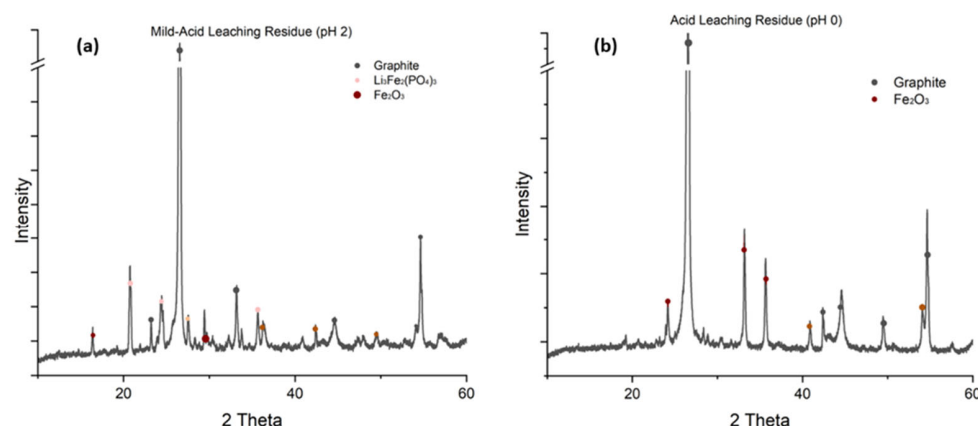


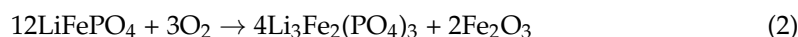
Figure 8. XRD patterns of solid residues after leaching under different pH conditions: (a) Solid residue after leaching at pH 2 (mild-acid leaching); (b) Solid residue after leaching at pH 0 (acid leaching).

4. Discussion

This study reveals a critical paradox in lithium iron phosphate (LFP) recycling: while oxidative roasting successfully transforms LiFePO_4 into water-soluble $\text{Li}_3\text{Fe}_2(\text{PO}_4)_3$ (Equation (1)), its benefits are overshadowed by the complex reality of industrial blackmass. Our results challenge the assumption that thermal pretreatment universally enhances lithium recovery, particularly when applied to real-world battery waste rich in graphite (~46%) and impurities (Al, Cu, and F).

4.1. Oxidative Roasting Mechanism and Phase Transformations

At 650 °C in air, LiFePO_4 undergoes oxidation to form water-soluble $\text{Li}_3\text{Fe}_2(\text{PO}_4)_3$ and Fe_2O_3 , as described by the following chemical Equation (2);



Concurrently, graphite combusted ($\text{C} + \text{O}_2 \rightarrow \text{CO}_2$), reducing the carbon content from 46.6% to 18.4% (Figure 2). This eliminates the carbon coatings too, exposing $\text{Li}_3\text{Fe}_2(\text{PO}_4)_3$ for efficient leaching, as seen in Figure 9. Binder decomposition (PVDF) above 350 °C also liberates adhered particles (Figure 5), while the residual fluorine drops from 2.3% to 1.3%, minimizing interference during leaching. At elevated temperatures, partial decomposition of $\text{Li}_3\text{Fe}_2(\text{PO}_4)_3$ occurs:

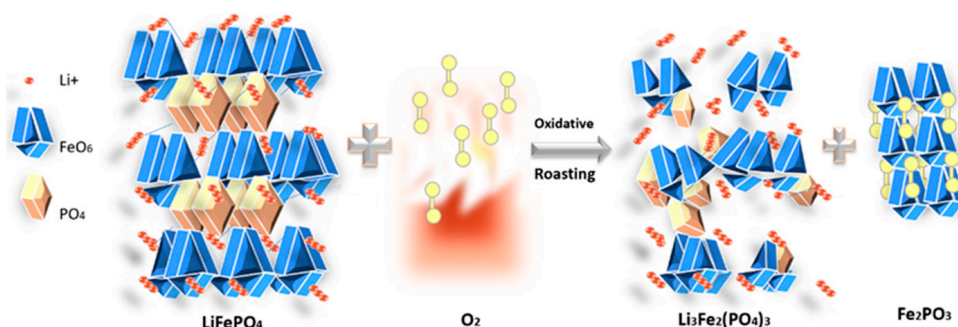
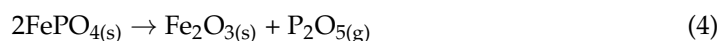
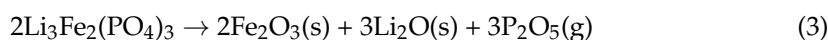
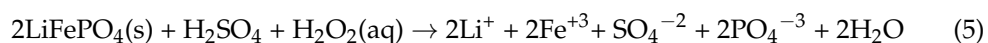


Figure 9. Illustrative description of oxidative roasting of LiFePO_4 .

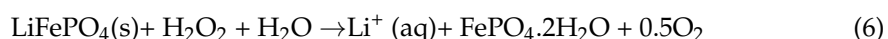
4.2. Selective Leaching Behavior

The effect of oxidative roasting on the leaching conditions (different pH values) was found to be beneficial for the maximization of Li leaching efficiency only at pH 0. In this situation, the concentration of H_2SO_4 is high, which enables the breaking of chemical bonds and promotes the liberation of each chemical element. The chemical reaction (4) occurs, and it is believed that a similar reaction involving the compound $\text{Li}_3\text{Fe}_2(\text{PO}_4)_3$ might also occur.



Although Fe is present in different compounds under the roasted and unroasted treatments, the leaching was considerably high, as well as for P, which means no Li selectivity was achieved. In addition, the presence of binders or any organic material is not hindered significantly at pH 0. However, it must be mentioned that the consumption of acid is high, which also brings a high concentration of sulfur to the wastewater. The sustainable and green approach is compromised in this alternative.

At both higher pH values of 5 and 9, the unroasted BM showed higher selectivity but poor Li extraction. According to the E-pH diagram of the pure LiFePO_4 compound, pH 9 is not favorable for the formation of ions. At pH 5 and in a high oxidation environment, selectivity is achieved. However, the leaching efficiency of Li is compromised, and does not reach 60%. The chemical reaction (5) might occur, which allows the recombination of Fe and PO_4 to form insoluble FePO_4 .



The best scenario is shown at pH 2, with a hint of H_2SO_4 and unroasted BM. In this case, the roasting of the LFP BM, while eliminating F and any possible binder or electrolyte that could hinder the leaching, shows a negative result in relation to the Li leaching efficiency but a good result in terms of selectivity, since Fe and P showed a percentage of nearly zero. The reason behind this might be connected to the compound $\text{Li}_3\text{Fe}_2(\text{PO}_4)_3$ or the formation of other Li-compounds undetected by XRD, which are insoluble. For a complete assessment, the thermodynamic behavior of these roasted phases must be investigated.

4.3. Impurity Behavior and Selectivity

Unroasted blackmass showed high Al/Cu leaching (up to 50%) due to PVDF-bound particles (Figure 6). Roasting reduced their dissolution by 70–80%, as Al oxidized to aluminum oxides and Cu formed stable oxides. This aligns with the E-pH diagrams [1], where neutral-to-alkaline conditions favor $\text{FePO}_4/\text{Li}_3\text{PO}_4$ stability, suppressing impurity solubility.

Several factors help explain why roasting underperformed. First, the high graphite content (about 46%) in our blackmass, while reduced during roasting, created a porous and reactive matrix that physically trapped lithium phosphate particles. This encapsulation limited the exposure of $\text{Li}_3\text{Fe}_2(\text{PO}_4)_3$ to the leaching solution, reducing the effectiveness of subsequent lithium extraction. Second, although roasting reduced the fluorine content by breaking down PVDF binders, some binder residues persisted, likely forming hydrophobic coatings that further hindered water penetration and lithium dissolution. Our SEM images supported this, showing agglomerated particles and uneven surfaces in the roasted residues.

Another important factor is the complexity of industrial blackmass itself. Unlike laboratory-prepared LFP cathodes, our material contained notable amounts of aluminum and copper. During roasting, these impurities formed stable oxides that may have adsorbed or trapped lithium ions, effectively locking them in the solid phase and making them less

accessible during leaching. This is supported by our leaching results, which showed that acid leaching could extract over 95% of the lithium but also dissolved significant amounts of iron and other impurities, undermining the selectivity and purity of the recovered lithium.

These findings challenge the common assumption that roasting always enhances lithium recovery, especially for real-world battery waste. Our results suggest that the benefits of roasting are highly dependent on the composition and structure of the feedstock, as indicated by Table 2. For high-graphite, impurity-rich blackmass, the energy and material costs of roasting may not be justified, especially when a similar lithium recovery can be achieved through direct hydrometallurgical processing. This insight points to the need for recycling protocols that are tailored to the specific characteristics of the input material, rather than relying on a one-size-fits-all approach.

Table 2. A comparison table showing LFP source, key parameters, and its recovery among the latest research.

Study	Feed Source	Li Recovery (%)	Fe/Li Molar Ratio	Key Parameters
Current Study	Industrial BM	33–95	0.24–0.97	H ₂ SO ₄ /H ₂ O ₂ , 20 °C, 40 g/L
Jing et al. [11]	Lab synthesized LFP	95.4	0.05	H ₂ O ₂ , neutral pH, 80 °C
Wang et al. [26]	Industrial BM	97	1.02	H ₂ SO ₄ , 60 °C
Zhang et al. [31]	Virgin LFP	98	1.10	H ₂ SO ₄ , 80 °C

5. Conclusions

Our work reveals a critical gap between lab-scale recycling studies and the industrial reality. While roasting transformed LiFePO₄ into water-soluble Li₃Fe₂(PO₄)₃ (Eq I), reducing the carbon content by 60% and fluorine (from PVDF) by 43%, the benefits were compromised by the blackmass inherent complexity. In our research, under optimized conditions (40 g/L solid/liquid ratio, 20 °C), water leaching (pH 2, water + H₂O₂ + Hint of H₂SO₄) achieved 33% lithium recovery much lower than unroasted LFP with 90%, while acid leaching (pH 0, 2M H₂SO₄ + H₂O₂) reached 95.4% efficiency, albeit with higher impurity dissolution.

These results highlight that the high graphite content, persistent PVDF residues, and the presence of aluminum and copper impurities can limit the effectiveness of roasting as a pretreatment step.

Our findings emphasize that recycling strategies must be tailored to the specific composition and complexity of real-world battery waste. For graphite-rich blackmass, direct hydrometallurgical processing may offer a more practical and sustainable solution than energy-intensive roasting.

Future work must prioritize kinetic studies to accelerate Li₃Fe₂(PO₄)₃ dissolution, low-temperature binder removal to avoid graphite pitfalls, and collaboration with manufacturers to reduce PVDF/Al in next-gen batteries. As LFP dominates the EV revolution, recycling innovation must embrace feedstock complexity because sustainability is not just about chemistry, but adaptability.

Supplementary Materials: The following supporting information can be downloaded at: <https://www.mdpi.com/article/10.3390/met15070739/s1>.

Author Contributions: Conceptualization, D.D.M. and A.T.; methodology, D.D.M. and A.T.; validation, D.D.M. and A.T.; formal analysis, D.D.M. and A.T.; investigation, A.T.; resources, D.D.M. and A.T.; writing—original draft preparation, D.D.M. and A.T.; writing—review & editing, R.Y., A.B. and B.F.; visualization, D.D.M. and A.T.; supervision, D.D.M., B.F. and R.Y.; project administration, A.B. and R.Y.; funding acquisition, R.Y. All authors have read and agreed to the published version of the manuscript.

Funding: This research received no external funding. The authors are responsible for the contents of this publication. A.T. was funded via a DAAD scholarship in the frame of the long-year TGGS-RWTH collaboration. The scholarship application was initiated by R.Y. All other costs were covered by the IME—RWTH Aachen University.

Data Availability Statement: The original contributions presented in this study are included in the article/Supplementary Materials. Further inquiries can be directed to the corresponding author.

Acknowledgments: The authors would like to express their gratitude to the materials characterization facility (XRD, SEM) at TGGS, Bangkok. We would also like to thank the analytical laboratory (ICP-OES) of the institute for their great teamwork.

Conflicts of Interest: The authors declare no conflicts of interest.

References

- Holzer, A.; Windisch-Kern, S.; Ponak, C.; Raupenstrauch, H. A Novel Pyrometallurgical Recycling Process for Lithium-Ion Batteries and Its Application to the Recycling of LCO and LFP. *Metals* **2021**, *11*, 149. [CrossRef]
- Billmann, L. *Comparative Study of Li-Ion Battery Recycling Processes*; ACCUREC Recycling GmbH: Krefeld, Germany, 2020.
- Biswas, J.; Ulmala, S.; Wan, X.; Partinen, J.; Lundström, M.; Jokilaakso, A. Selective Sulfation Roasting for Cobalt and Lithium Extraction from Industrial LCO-Rich Spent Black Mass. *Metals* **2023**, *13*, 358. [CrossRef]
- Forte, F.; Pietrantonio, M.; Pucciarmati, S.; Puzone, M.; Fontana, D. Lithium iron phosphate batteries recycling: An assessment of current status. *Crit. Rev. Environ. Sci. Technol.* **2020**, *51*, 2232–2259. [CrossRef]
- Gaines, L.; Richa, K.; Spangenberg, J. Key issues for Li-ion battery recycling. *MRS Energy Sustain.* **2018**, *5*, 12. [CrossRef]
- Gonzalez, M.D.M.; Villen-Guzman, M.; Vereda, C.; Rodríguez-Maroto, J.; Paz-García, J. Towards Sustainable Lithium-Ion Battery Recycling: Advancements in Circular Hydrometallurgy. *Processes* **2024**, *12*, 1485. [CrossRef]
- Greil, R.; Chai, J.; Rudelstorfer, G.; Mitsche, S.; Lux, S. Water as a Sustainable Leaching Agent for the Selective Leaching of Lithium from Spent Lithium-Ion Batteries. *ACS Omega* **2024**, *9*, 7806–7816. [CrossRef]
- Haynes, W.M. (Ed.) *CRC Handbook of Chemistry and Physics*, 97th ed.; CRC Press: Boca Raton, FL, USA, 2016. [CrossRef]
- Liang, Z.; Cai, C.; Peng, G.; Hu, J.; Hou, H.; Liu, B.; Liang, S.; Xiao, K.; Yuan, S.; Yang, J. Hydrometallurgical recovery of spent lithium-ion batteries: Environmental strategies and sustainability evaluation. *ACS Sustain. Chem. Eng.* **2021**, *9*, 6105–6116. [CrossRef]
- Jie, Y.; Yang, S.; Li, Y.; Zhao, D.; Lai, Y.; Chen, Y. Oxidizing roasting behavior and leaching performance for the recovery of spent lifepo4 batteries. *Minerals* **2020**, *10*, 949. [CrossRef]
- Jin, H.; Zhang, J.; Wang, D.; Jing, Q.; Chen, Y.; Wang, C. Facile and efficient recovery of lithium from spent LiFePO₄ batteries via air oxidation–water leaching at room temperature. *Green Chem.* **2022**, *24*, 152–162. [CrossRef]
- Kasuno, T.; Kitada, A.; Shimokawa, K.; Murase, K. Suppression of Silver Dissolution by Contacting Different Metals during Copper Electrowinning. *J. MMIJ* **2014**, *130*, 65–69. [CrossRef]
- Lai, Y.; Zhu, X.; Xu, M.; Li, J.; Wang, R.; Zhou, Y.; Zhu, Y.; Zhu, X.; Liao, Q. Recycling of spent LiFePO₄ batteries by oxidizing roasting: Kinetic analysis and thermal conversion mechanism. *J. Environ. Chem. Eng.* **2023**, *11*, 110799. [CrossRef]
- Larouche, F.; Tedjar, F.; Amouzegar, K.; Houlachi, G.; Bouchard, P.; Demopoulos, G.P.; Zaghbi, K. Progress and Status of Hydrometallurgical and Direct Recycling of Li-Ion Batteries and Beyond. *Materials* **2020**, *13*, 801. [CrossRef] [PubMed]
- Li, J.; Zhang, J.; Zhao, W.; Lu, D.; Ren, G.; Tu, Y. Application of Roasting Flotation Technology to Enrich Valuable Metals from Spent LiFePO₄ Batteries. *ACS Omega* **2022**, *7*, 25590–25599. [CrossRef] [PubMed]
- Li, P.; Luo, S.; Zhang, L.; Liu, Q.; Wang, Y.; Lin, Y.; Xu, C.; Guo, J.; Cheali, P.; Xia, X. Progress, challenges, and prospects of spent lithium-ion batteries recycling: A review. *J. Energy Chem.* **2024**, *89*, 144–171. [CrossRef]
- Li, Z.; Zheng, Q.; Nakajima, A.; Zhang, Z.; Watanabe, M. Organic Acid-Based Hydrothermal Leaching of LiFePO₄ Cathode Materials. *Adv. Sustain. Syst.* **2024**, *8*, 2300421. [CrossRef]
- Liu, G.; Liu, Z.; Gu, J.; Yuan, H.; Wu, Y.; Chen, Y. A facile new process for the efficient conversion of spent LiFePO₄ batteries via (NH₄)₂S₂O₈-assisted mechanochemical activation coupled with water leaching. *Chem. Eng. J.* **2023**, *471*, 144265. [CrossRef]
- Ma, X.; Ge, P.; Wang, L.; Sun, W.; Bu, Y.; Sun, M.; Yang, Y. The Recycling of Spent Lithium-Ion Batteries: Crucial Flotation for the Separation of Cathode and Anode Materials. *Molecules* **2023**, *28*, 4081. [CrossRef]
- Müller, M.; Obuz, H.E.; Keber, S.; Tekmanli, F.; Mettke, L.N.; Yagmur, B. Concepts for the Sustainable Hydrometallurgical Processing of End-of-Life Lithium Iron Phosphate (LFP) Batteries. *Sustainability* **2024**, *16*, 11267. [CrossRef]
- European Parliamentary Research Service. New EU Regulatory Framework for Batteries: Setting Sustainability Requirements. *Briefing*, 5 September 2024. Available online: [https://www.europarl.europa.eu/thinktank/en/document/EPRS_BRI\(2021\)689337](https://www.europarl.europa.eu/thinktank/en/document/EPRS_BRI(2021)689337) (accessed on 23 May 2025).

22. Obuz, H.; Tekmanlı, F.; Mettke, L.; Müller, M.; Yagmurlu, B. Investigation of Recycling Behavior of Lithium Iron Phosphate Batteries with Different Thermal Pre-Treatments. *Mater. Proc.* **2023**, *15*, 68. [\[CrossRef\]](#)
23. Li, H.; Xing, S.; Liu, Y.; Li, F.; Guo, H.; Kuang, G. Recovery of lithium, iron, and phosphorus from spent LiFePO_4 batteries using stoichiometric sulfuric acid leaching system. *ACS Sustain. Chem. Eng.* **2017**, *5*, 7350–7358. [\[CrossRef\]](#)
24. Seo, B.; Park, H.-K.; Na, T.; Heo, S.; Kim, R.; Yoon, H.-S.; Chung, K.W.; Park, K. Selective leaching behavior of Nd from spent NdFeB magnets treated with combination of selective oxidation and roasting processes. *Hydrometallurgy* **2024**, *227*, 106320. [\[CrossRef\]](#)
25. Stallmeister, C.; Friedrich, B. Holistic Investigation of the Inert Thermal Treatment of Industrially Shredded NMC 622 Lithium-Ion Batteries and Its Influence on Selective Lithium Recovery by Water Leaching. *Metals* **2023**, *13*, 2000. [\[CrossRef\]](#)
26. Wang, D.-F.; Chen, M.; Zhao, J.-J.; Zhou, F.-Y.; Wang, H.-Y.; Qu, X.; Cai, Y.-Q.; Zheng, Z.-Y.; Wang, D.-H.; Yin, H.-Y. Revealing role of oxidation in recycling spent lithium iron phosphate through acid leaching. *Rare Met.* **2025**, *44*, 2059–2070. [\[CrossRef\]](#)
27. Woeste, R.; Drude, E.-S.; Vrucak, D.; Klöckner, K.; Rombach, E.; Letmathe, P.; Friedrich, B. A techno-economic assessment of two recycling processes for black mass from end-of-life lithium-ion batteries. *Appl. Energy* **2024**, *361*, 122921. [\[CrossRef\]](#)
28. Xu, Y.; Zhang, B.; Ge, Z.; Zhang, S.; Song, B.; Tian, Y.; Deng, W.; Zou, G.; Hou, H.; Ji, X. Advances and perspectives towards spent LiFePO_4 battery recycling. *J. Clean. Prod.* **2024**, *434*, 140077. [\[CrossRef\]](#)
29. Yang, C.; Zhang, J.; Jing, Q.; Liu, Y.; Chen, Y.; Wang, C. Recovery and regeneration of LiFePO_4 from spent lithium-ion batteries via a novel pretreatment process. *Int. J. Miner. Metall. Mater.* **2021**, *28*, 1478–1487. [\[CrossRef\]](#)
30. Zhang, L.; Teng, T.; Xiao, L.; Shen, L.; Ran, J.; Zheng, J.; Zhu, Y.; Chen, H. Recovery of LiFePO_4 from used lithium-ion batteries by sodium-bisulphate-assisted roasting. *J. Clean. Prod.* **2022**, *379*, 134748. [\[CrossRef\]](#)
31. Zhang, Y.; Ru, J.; Hua, Y.; Cheng, M.; Lu, L.; Wang, D. Priority Recovery of Lithium From Spent Lithium Iron Phosphate Batteries via H_2O -Based Deep Eutectic Solvents. *Carbon Neutralization* **2025**, *4*, e186. [\[CrossRef\]](#)
32. Zhang, G.; Yuan, X.; Tay, C.Y.; He, Y.; Wang, H.; Duan, C. Selective recycling of lithium from spent lithium-ion batteries by carbothermal reduction combined with multistage leaching. *Sep. Purif. Technol.* **2023**, *314*, 123555. [\[CrossRef\]](#)
33. Zhao, T.; Marthi, R.; Mahandra, H.; Chae, S.; Traversy, M.; Sadri, F.; Choi, Y.; Ghahreman, A. Direct selective leaching of lithium from industrial-grade black mass of waste lithium-ion batteries containing LiFePO_4 cathodes. *Waste Manag.* **2023**, *171*, 134–142. [\[CrossRef\]](#)
34. Zheng, R.; Zhao, L.; Wang, W.; Liu, Y.; Ma, Q.; Mu, D.; Li, R.; Dai, C. Optimized Li and Fe recovery from spent lithium-ion batteries via a solution-precipitation method. *RSC Adv.* **2016**, *6*, 43613–43625. [\[CrossRef\]](#)

Disclaimer/Publisher’s Note: The statements, opinions and data contained in all publications are solely those of the individual author(s) and contributor(s) and not of MDPI and/or the editor(s). MDPI and/or the editor(s) disclaim responsibility for any injury to people or property resulting from any ideas, methods, instructions or products referred to in the content.